Supporting Information

Topotactic BI_3-assisted borodization: Synthesis and electrocatalysis applications of transition metal borides

Katherine E. Woo,[a,b,#] Seongyoung Kong,[a,b,#] Wei Chen,[c,#] Tsz Hin Chang,[d] Gayatri Viswanathan,[a,b] Aida M. Díez,[e] Viviana Sousa,[e] Yury V. Kolen'ko,[e] Oleg I. Lebedev,[f] Marta Costa Figueiredo,[c,*] Kirill Kovnir [a,b,*]

[a] *Department of Chemistry, Iowa State University, Ames, Iowa 50011, USA*

[b] *Ames Laboratory, U.S. Department of Energy, Ames, Iowa 50011, USA*

[c] *Department of Chemical Engineering and Chemistry, Eindhoven University of Technology, 5600 MB Eindhoven, Netherlands*

[d] *Department of Chemistry, University of California, Davis, Davis, California, 95616, USA*

[e] *Nanochemistry Research Group, International Iberian Nanotechnology Laboratory, Braga 4715-330, Portugal*

[f] *Laboratoire CRISMAT, ENSICAEN, CNRS UMR 6508, 14050 Caen, France*

# These authors contributed equally

** Corresponding authors: m.c.costa.figueiredo@tue.nl, kovnir@iastate.edu*

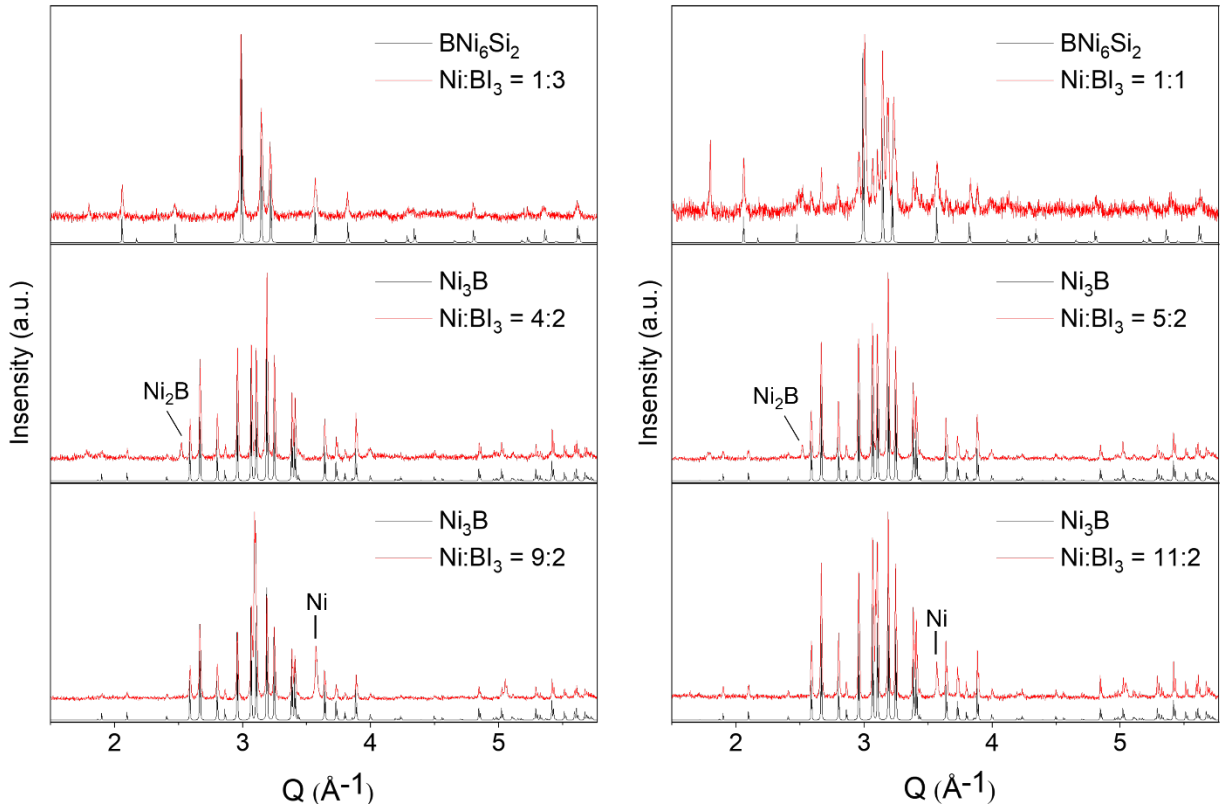

Figure S1. Powder XRD patterns (red) of reactions targeting nickel boride (Ni_3B) using different $Ni:BI_3$ ratios as detailed in **Table 2**. The calculated pattern (black) was assigned as the major phase of the product. The most intense peak of the admixture phase is indicated with corresponding composition.

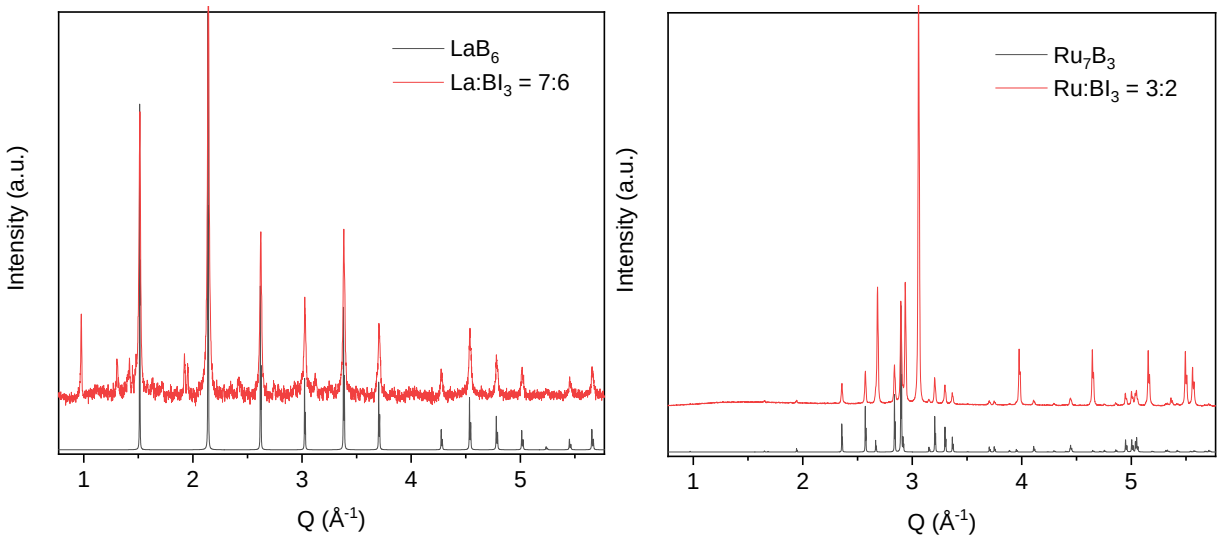

Figure S2. Calculated (black) and experimental (red) powder XRD patterns for reactions targeting LaB_6 and Ru_7B_3 with given ratios of *M*:BI_3. Majority of the unassigned peaks in Ru_7B_3 correspond to unreacted Ru metal.

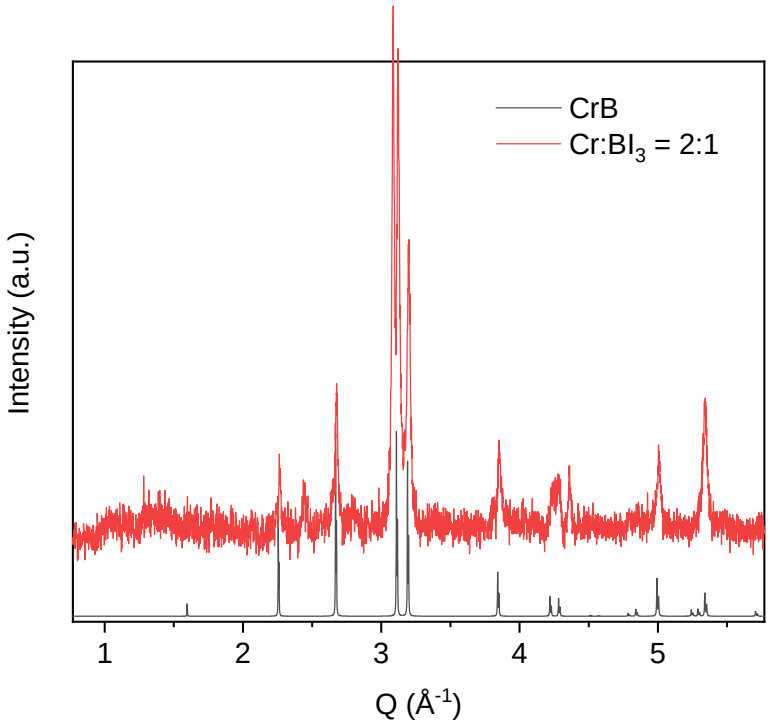

Figure S3. Calculated (black) powder XRD pattern of CrB and experimental pattern (red) synthesized by given *M*:BI_3 ratio.

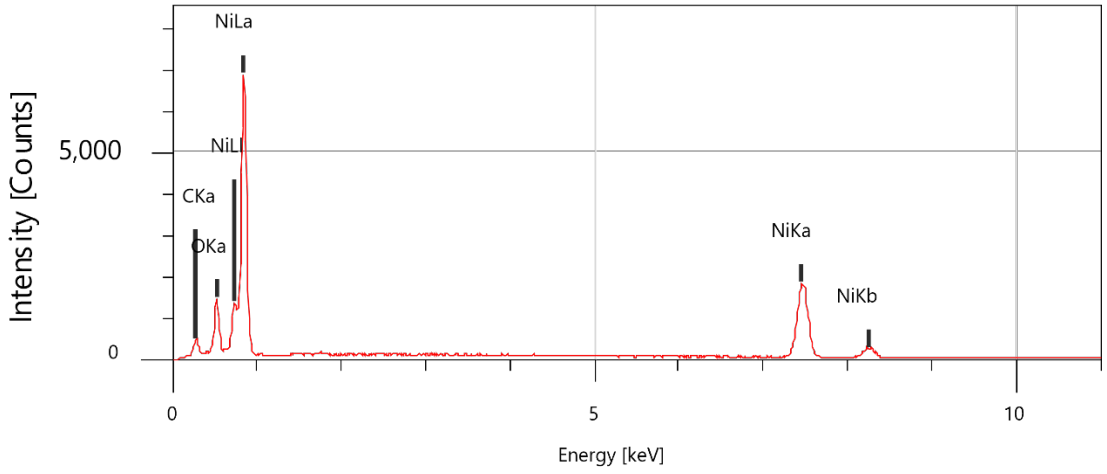

Figure S4. EDX spectrum of Ni_3B foam after washing with water. No iodine was detected. B-K_α peak overlaps with that of C.

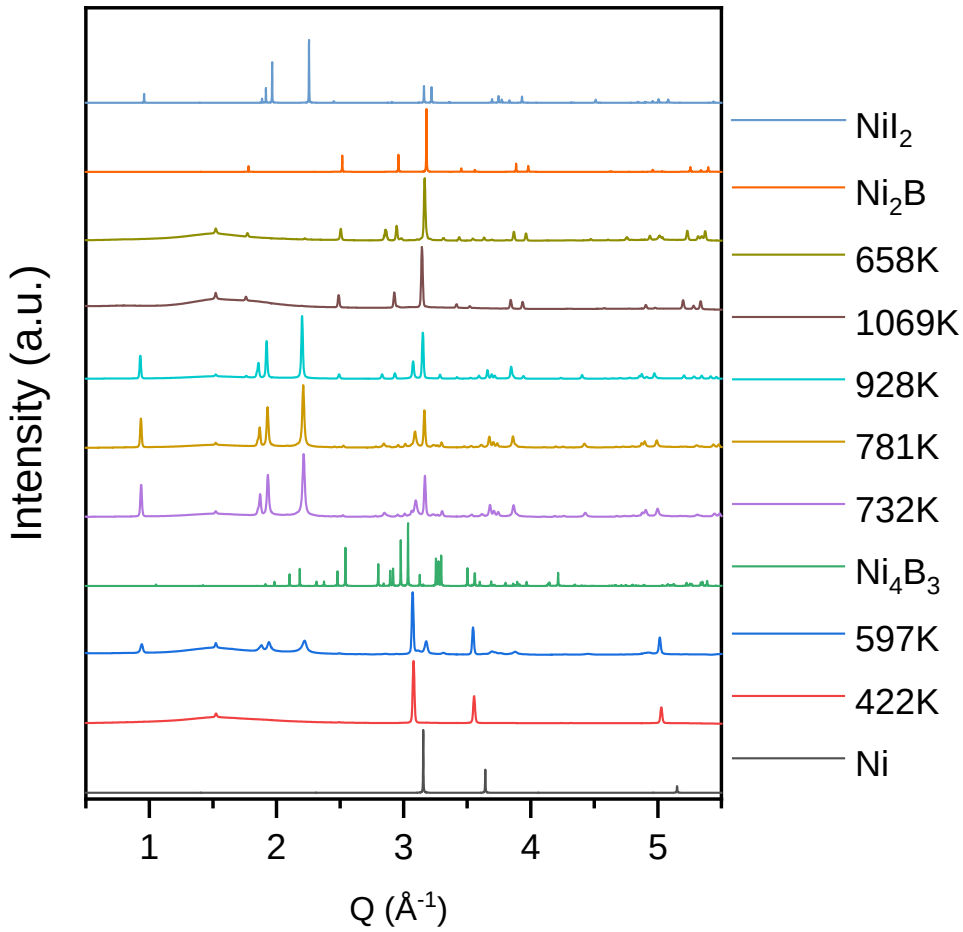

Figure S5. Selected *in situ* powder XRD patterns of the Ni and BI_3 reaction at the representative temperature regions and calculated XRD patterns of Ni, Ni_4B_3 Ni_2B and NiI_2. A trend of peak shifts is due to thermal expansion of the unit cell.

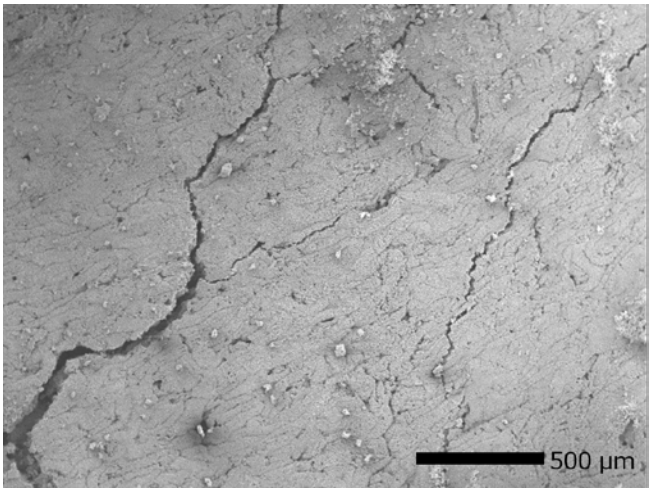

Figure S6. SEM backscattered electron image of Ni_3B foam with morphology lacking pores.

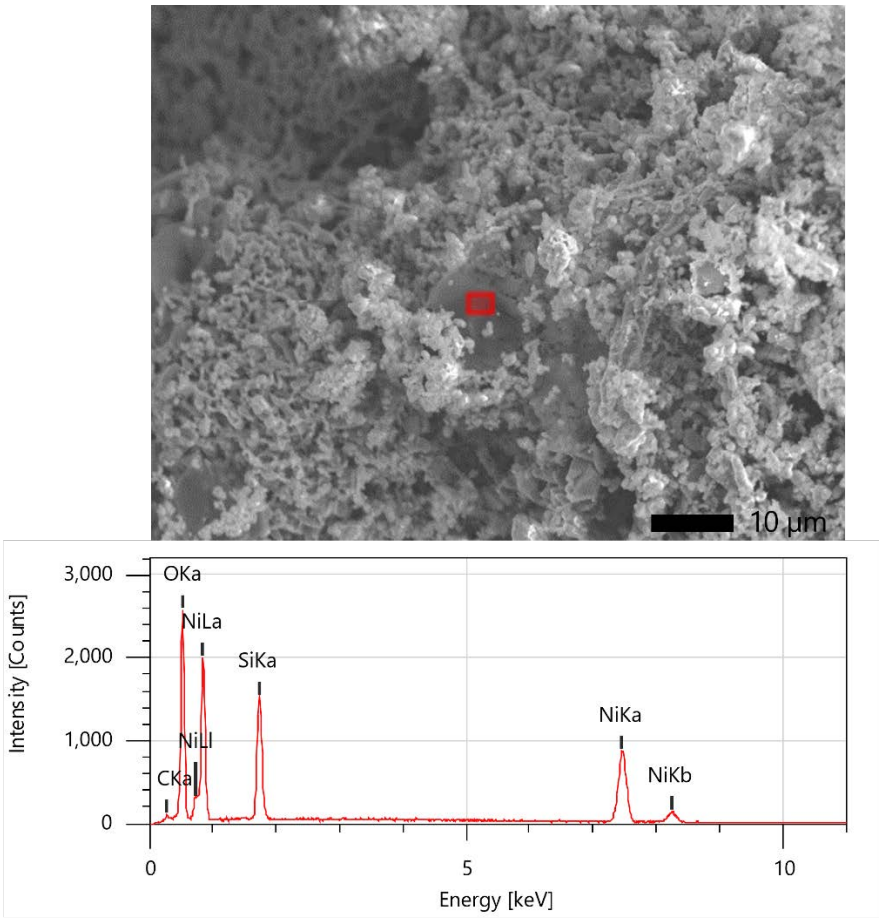

Figure S7. SEM backscattered electron image and EDX spectrum ofNi_6BSi_2 crystal on the Ni_3B form. B-K_α peak overlaps with that of C.

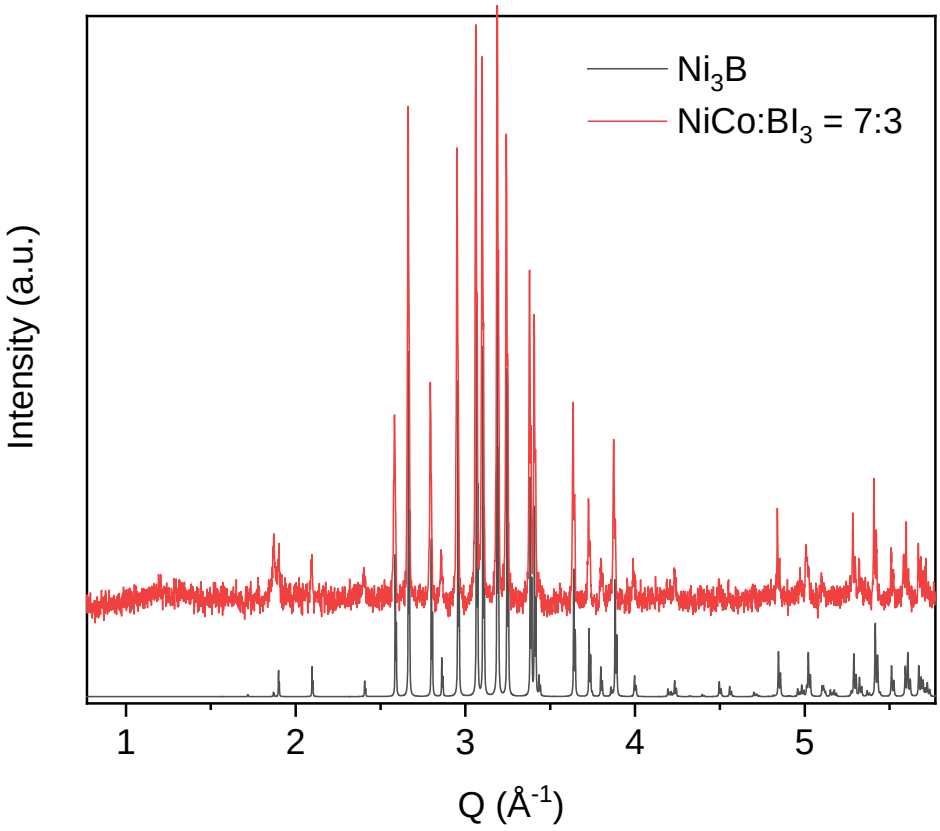

Figure S8. Calculated (black) powder XRD pattern of Ni_3B and experimental (red) pattern of $Ni_{2.1(1)}Co_{0.9}B$.

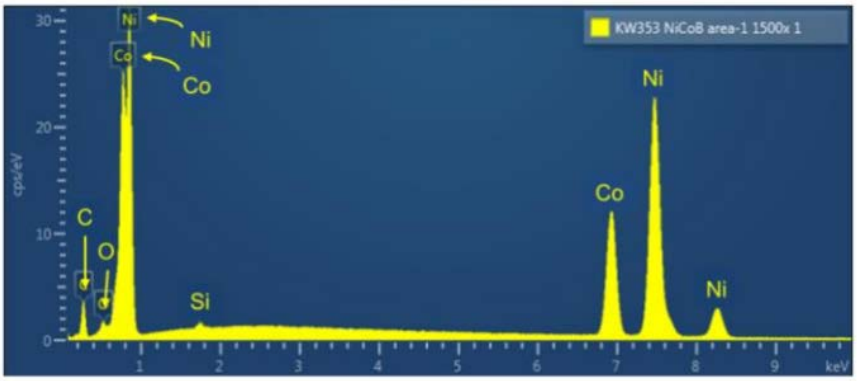

Figure S9. EDX spectrum of ternary $Ni_{2.1(1)}Co_{0.9}B$. B-K_α peak overlaps with that of C.

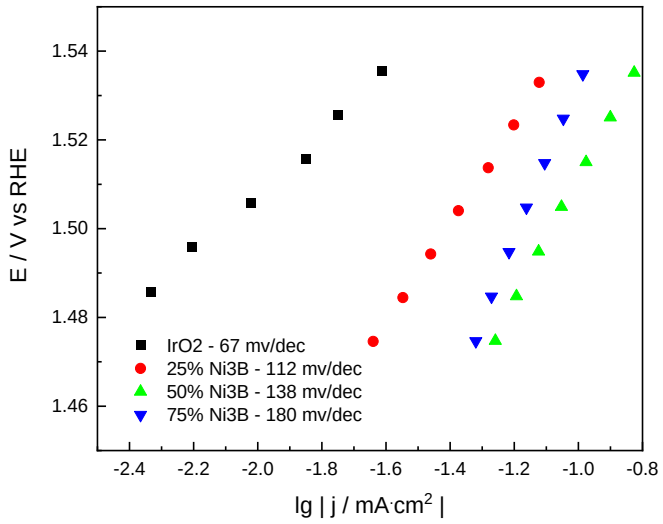

Figure S10. Tafel plots for IrO_2 and IrO_2/Ni_3B catalysts with different compositions. Data obtained in N_2 saturated 0.5 M H_2SO_4. (mass loading = 0.25 mg/cm^2).

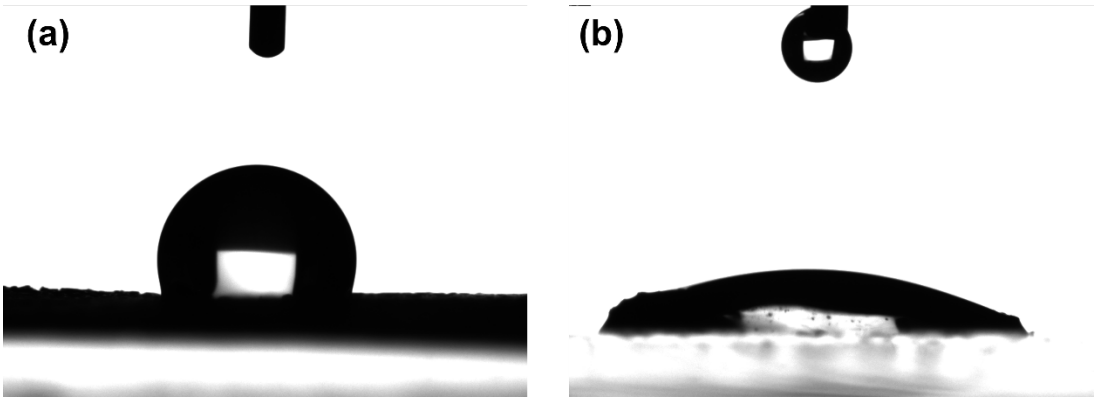

Figure S11. Contact angle study showing water droplet on the surface of (a) Ni foam and (b) Ni_3B foam.

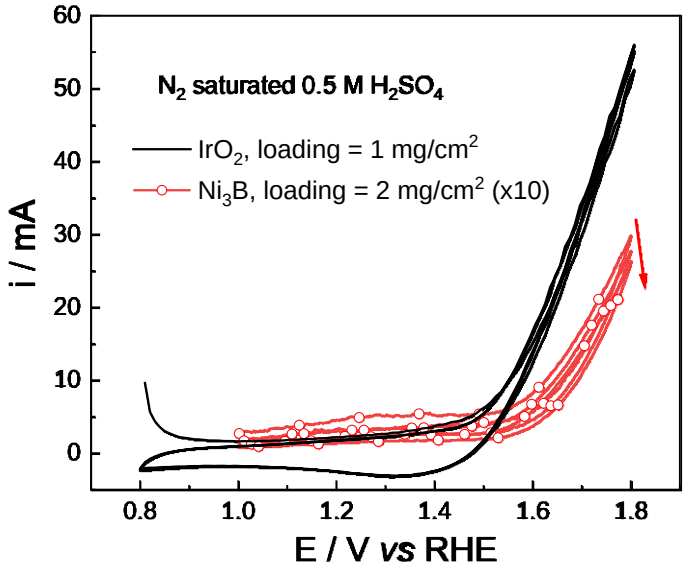

Figure S12. Cyclic voltammogram of IrO_2 (loading = 1 mg/cm^2) and Ni_3B (loading = 2 mg/cm^2) in N_2 saturated 0.5 M H_2SO_4. Scan rate = 50 mv/s, electrode rotating rate = 1600 rpm. The initial three cycles are given without *iR* compensation. For better comparison, the loading of Ni_3B has been doubled and the corresponding current has been multiplied by 10.

Table S1. Overpotentials for pure IrO_2 and IrO_2/Ni_3B with different compositions to generate j_{ECSA} = 0.4 mA/cm^2 (mass loading = 0.25 mg/cm^2).

	E/V @ 0.4mA/cm^2	**Overpotential/mV**
IrO_2 100%	1.67	440
Ni_3B 25% /IrO_2 75%	1.65	420
Ni_3B 50% /IrO_2 50%	1.60	370
Ni_3B 75% /IrO_2 25%	1.63	400